Possible mechanism for fractional and negative magnetic flux in mesoscopic superconductors

Shi-Ping Zhou, Yao-Ming Shi, Bao-He Zhu, and Guo-Qiao Zha
Department of Physics, Shanghai University, Shanghai 200436, China
(Received 27 October 2005; revised manuscript received 23 February 2006; published 5 May 2006)

We study vortex state transitions of mesoscopic superconducting disks using the Bogolubov-de Gennes equations. A vortex charge associated spin-orbit interaction is considered. This interaction induces an additional geometric phase and an intrinsic energy barrier for state transition of a different angular quantum number, leading to metastablility. This provides possible interpretations for experimental observations of the noninteger flux quanta and negative flux jump in mesoscopic superconductors [Geim *et al.*, Nature (London) **407**, 55 (2000)].

DOI: 10.1103/PhysRevB.73.174503 PACS number(s): 74.20.De, 73.23.−b

I. INTRODUCTION

The flux carried by vortices differing from an integer multiple of flux quanta $\Phi_0 \equiv hc/2e$ and the "negative vortex" whose penetration leads to the expulsion of magnetic field have been experimentally[1] shown for mesoscopic superconductors with the size comparable to the superconducting coherence length ξ and/or the magnetic field penetration depth λ. The phenomenological Ginzburg-Landau theory has been used extensively to describe the unusual phenomena.[2–8] The surface barrier[2,5,6] based on Bean-Livingston (BL) model[9] is supposed to be responsible for the experimental findings. According to the BL model, a surface barrier exists due to the competition between the vortex attraction by its mirror image (outside of the sample) and its repulsion by the near-edge screening currents. Vortices can then initially penetrate only at a finite distance from the edge, and the amount of flux varies on their distance from the sample edge and can be smaller than Φ_0, as first pointed out by Bardeen[10] and Ginzburg.[11] It is, however, obvious that this argument seems not so sound for the negative flux jump. In addition, the BL model is essentially based on the London theory, which is then valid only for the vortex motion far from the sample boundary that is inconsistent with the mesoscopic case. We will show that these abnormalities would be closely related to how the charged vortices distribute and their dynamics as well.[15–22] Khomskii and Freimuth[16] suggested that the vortex core should be charged up due to the chemical potential in the superconducting state breaking the particle-hole symmetry different from that in the normal state. In addition, Hayashi *et al.*[18] showed that vortices are intrinsically charged up in superconductors having a small value of $k_F\xi$. This vortex charge together with the screening effect[12] determines the microscopic electron structure and the dynamics of the vortex.[20,21] The charged vortices induce an electrostatic field, which in turn generates a spin-orbit (SO) term that becomes appreciably larger for mesoscopic superconductors due to the quantum size effect. It is, therefore, essential to include the vortex charging induced electrostatic field in order to account for experimental findings.[1]

In this work, we perform studies for the BdG equations[14] invoking the charge redistribution associated SO coupling contribution. We find that the SO interaction can give rise to an additional Aharonov-Casher (AC)-like[22] phase to the wave function of electrons (holes). A noninteger flux quanta is then expected since wave function phase must be quantized. In addition, we show that the spin-orbit term can induce a barrier that depresses the presumably first-order transition between the giant vortex states of different angular quantum numbers, resulting in metastability that closely ties to the negative flux jump as state transition occurs with increasing field.

II. THE MODEL

A type-II superconductor in the mixed state can be treated as a system with two electronic subsystems, one of which is superconducting, the other with the core size in the order of coherence length ξ remains the normal.[23] The transition of a system to a superconducting state leads to a chemical potential change $\delta\mu(\vec{r})$ for the electrons (holes) of these subsystems, which makes charge redistribution and vortices charging up.[16] The position-dependent chemical potential change requires an electrostatic potential $\varphi_{es}(\vec{r})$ so that the electrochemical potential (for electrons in a metal) $\mu_{el}=\mu_0+\delta\mu(\vec{r})+e\varphi_{es}(\vec{r})$ is spatially constant, which then induces an electric field defined as $\vec{E}=-\text{grad}(\varphi_{es})$. Here, the electrostatic potential expressed in terms of the normalized order parameters $\tilde{\psi}\equiv\psi/\psi_0$ as[15] $\varphi_{es}=\tilde{\varphi}_0(\tilde{\psi}\cdot\tilde{\psi}^*-1)$ with $\tilde{\varphi}_0\simeq\tilde{c}|\alpha|/2\pi^2e$, $|\alpha|=\hbar^2/4m\xi^2$ and $\tilde{c}\sim(1-10)$. The dimensionless wave function of the particle of charge $2e$, e.g., a Cooper pair, is associated with the pair potential $\Delta(\vec{r})$ by[14] $\tilde{\psi}=(8.392\tilde{n}/8\pi^2k_B^2T_C^2)^{1/2}\Delta(\vec{r})/\psi_0$, whereas $\psi_0^2=\tilde{n}/4$ with $\tilde{n}$ the total electron number per cubic centimeter. Hence, the electric field reads

$$\vec{E}=\frac{1}{e}\frac{\hbar^2}{m\xi^2}\frac{8.392}{8\pi^2k_B^2T_C^2}|\Delta|\text{grad}(|\Delta|). \tag{1}$$

(We have chosen $\tilde{c}=10$.) This induced field acts on the quasiparticle of spin $\vec{\sigma}$, mass m, and charge e adding a spin-orbit coupling term $\hat{H}_{so}\equiv-e\hbar/4m^2c^2\hat{\sigma}\cdot\vec{E}\times(-i\hbar\nabla-e/c\vec{A})$ to the Hamiltonian of the system. The Bogolubov-de Gennes equations[14] then read

$$\varepsilon_i u_i=(H_e+U+H_{so})u_i+\Delta v_i$$

$$\varepsilon_i v_i = -(H_e^* + U + H_{so}^*)v_i + \Delta^* u_i, \tag{2}$$

where the single electron energy measured from Fermi level E_F is $H_e \equiv \hat{p}^2/2m - E_F = 1/2m(-i\hbar\nabla - e/c\vec{A})^2 - E_F$. The index i denotes all quantum numbers. Note that the effective crystal potential $U(r)$ is an integral involving all states below the Fermi level and is nearly independent of temperature. By neglecting its details, the effective potential can be treated as a constant for a homogenous sample and it is assumed to be null for simplicity. The pair potential and the current density expressed in terms of the solutions of Eq. (2) as

$$\Delta(\vec{r}) = V \sum_{E_i \leqslant \hbar\omega_D} u_i(\vec{r}) v_i^*(\vec{r})[1 - 2f(\varepsilon_i)], \tag{3}$$

$$\vec{j}(\vec{r}) = \frac{e\hbar}{2mi}\sum_i \left[f(\varepsilon_i) u_i^* \left(\nabla - \frac{ie}{\hbar c}\vec{A} \right) u_i + [1 - f(\varepsilon_i)] v_i \left(\nabla - \frac{ie}{\hbar c}\vec{A} \right) v_i^* - \text{H.c.} \right], \tag{4}$$

where $g \equiv N(0)V$ is the coupling constant that describes the electron-electron attractive interaction, ω_D is the Debye frequency, and $f(E)$ is the Fermi distribution. The vector potential $\vec{A}$ is related to the current density $\vec{j}$ by Maxwell's equation

$$\nabla \times \nabla \times \vec{A} = \frac{4\pi}{c}\vec{j}, \tag{5}$$

and the boundary conditions are: $(\nabla \times \vec{A})|_s = \vec{H}_{ext}$, and $[\vec{n}(\nabla - ie/\hbar c\vec{A})\Delta(\vec{r})]|_s = 0$. A self-consistent solution is obtained by repeatedly solving Eq. (2) and calculating Δ and $\vec{A}$ using Eqs. (3)–(5). The parameters used in our computations are $E_F \sim 2m\xi_0^2\pi^2\Delta_0^2(0)/4\hbar^2 \sim 103$ meV, $g = 0.166$, $\omega_D = 35$ meV, and $T_c = 1.25$ K, $\Delta_0(0) \approx 0.345$ meV, $\xi_0 = 210$ nm for an *Al* superconductor.[14]

III. RESULTS AND DISCUSSIONS

A. The ac-like phase due to the spin-orbit interaction

We consider first the giant vortex state case where the system is expected invariant under rotations about the z axis, that is, the symmetric axis of the thin disc. We use the cylindrical coordinates (r, θ, z). For a thin disc of thickness $h \sim 0.1\xi_0$, the pair potential may be thought uniform along the z axis. Hence, only the radial component of electric field E_r and the angular component of the vector potential A_θ, and thereby the third component of the spin-orbit contribution is necessary to be involved. The SO term reduces to $H_{so} = -e\hbar/4m^2c^2\sigma_z \cdot \vec{E}_r(-i\hbar\nabla - e/c\vec{A})_\theta$ with $\sigma_z = \left(\begin{smallmatrix} 1 & 0 \\ 0 & -1 \end{smallmatrix}\right)$. We then have,

$$\left[\frac{\hat{p}^2}{2m} + \frac{e\hbar E_r}{4m^2c^2}\sigma_z \hat{p}_\theta \right] u_n + \Delta(\vec{r}) v_n = \varepsilon_n u_n,$$

$$-\left[\frac{\hat{p}^2}{2m} + \frac{e\hbar E_r}{4m^2c^2}\sigma_z \hat{p}_\theta \right] v_n + \Delta^*(\vec{r}) u_n = \varepsilon_n v_n, \tag{6a}$$

which break up into two independent matrix equations due to the spin-orbit coupling, one for the spin-up electron and spin-down hole quasiparticle wave function $\hat{\psi}_\uparrow \equiv (u_\uparrow, v_\downarrow)^T$, whereas another one $\hat{\psi}_\downarrow \equiv (u_\downarrow, v_\uparrow)^T$ for the spin-down electron and spin-up hole quasiparticle wave function. Each matrix equation has the same form, and we consider the $\hat{\psi}_\uparrow \equiv (u_\uparrow, v_\downarrow)^T$.

$$\begin{bmatrix} \frac{\hat{p}^2}{2m} + \frac{e\hbar E_r}{4m^2c^2}\hat{p}_\theta - E_F & \Delta \\ \Delta^* & -\left(\frac{\hat{p}^2}{2m} - \frac{e\hbar E_r}{4m^2c^2}\hat{p}_\theta \right)^* - E_F \end{bmatrix} \begin{pmatrix} u_\uparrow \\ v_\downarrow \end{pmatrix} = \varepsilon \begin{pmatrix} u_\uparrow \\ v_\downarrow \end{pmatrix}. \tag{6b}$$

Therefore, one can rewrite the kinematical momentum of the quasiparticle as $\hat{p} \pm \mu_q(\hat{z} \times \vec{E}_r)/c$ with $\mu_q = e\hbar/4mc$ for the spin-up electron or the spin-down hole. Denote $\vec{A}' = \vec{A} \mp (\mu_q/e)(\hat{z} \times \vec{E}_r)$ and $E_F' = E_F - (E_r\mu_q/c)^2$. Above kinematical momentum reduces to $-i\hbar\vec{\nabla} - (e/c)\vec{A}'$ that has a formal analogy with the kinematical momentum of a particle of charge e and mass m circulating around the magnetic field $\vec{h} = \nabla \times \vec{A}'$, and Eq. (6) then analog with the standard BdG equations. For convenience, we drop the superscript prime notation in the following discussions.

We introduce then the gauge-invariant theorem. Suppose that ε_n is an eigenvalue and $(u_n\ v_n)^T$ is the eigenfunction set for Eq. (6) with $\vec{A}$ and pair potential Δ. Then, $[u_n \exp(ie\chi/\hbar c)\ v_n \exp(-ie\chi/\hbar c)]^T$ is an eigenfunction set corresponding to the eigenvalue ε_n for Eq. (6) with $\vec{A} \to \vec{A} + \nabla\chi(\vec{r})$ and $\Delta \to \Delta \exp(2ie\chi/\hbar c)$ for a nonsingular scalar function χ.[24]

We choose $\vec{A} + \nabla\chi(\vec{r}) = 0$ to eliminate the potential vector from Eq. (6). The total magnetic flux $\Delta\chi$ is then given by

$$\Delta\chi = \oint_{\vec{l}=r\hat{\theta}} \vec{A} \cdot d\vec{l} + (\mu_q/e) \oint_{\vec{l}=r\hat{\theta}} (\vec{E}_r \times d\vec{l})\hat{z} \equiv \Phi(r) + \Phi_{SO}(r), \tag{7a}$$

where $\Phi(r)$ stands for the magnetic flux penetrating in the sample when $r \to a^-$, whereas

$$\Phi_{SO}(r) \equiv (\mu_q/e) \oint_{\vec{l}=r\hat{\theta}} (\vec{E}_r \times d\vec{l})\hat{z} = (\mu_q/e) \int\int_{s=\pi r^2} \nabla \cdot \vec{E}_r ds \tag{7b}$$

is the flux due to the SO interaction. It follows from the gauge-invariant theorem that $(u\ v)$ changes by a phase to $(ue^{+i(e/c\hbar)\Delta\chi}\ ve^{-i(e/c\hbar)\Delta\chi})$, and Δ to $\Delta \exp(2ie\Delta\chi/\hbar c)$, as the local electron coordinates $\vec{r}$ goes one turn around the sample. Clearly, the phase shift consists of two parts. One of them is

the Aharonov-Bohm (AB)-like[31] phase that describes the effect of a charged particle in the magnetic field $\nabla \times \vec{A}$. The other is the ac-like phase that comes from the SO interaction, i.e., as a result of a coupling of the spin current to an effective tensor gauge potential that is directly proportional to the electric field $\vec{E}$ along the path of the particle. We choose $\hat{\psi}_{n,\mu}(r,\theta)=[u_{n,\mu,k}(r)e^{i(\mu+n_q/2)\theta}v_{n,\mu,k}(r)e^{i(\mu-n_q/2)\theta}]^T$. The single-valued $\hat{\psi}_{\mu,k}(r,\theta)$ then requires that

$$(\mu \pm n_q/2)\cdot 2\pi \pm e\,(\Delta\chi)|_r/c\hbar = 2\pi n, \tag{8}$$

where n is an integer that is defined as the total angular quantum number of quasiparticles. μ is half and odd integers, whereas the integer n_q represents the angular quantum number for the mass center of the paired quasiparticles with wave function $(u\ v)$, and the integer k the radial quantum number. Therefore, the AB-like magnetic flux $\Phi(\vec{r})|_{r\to a^-}$ is quantized (in units of Φ_0) when the SO contribution Φ_{SO} is negligible, whereas a sufficiency large contribution from the SO interaction would lead to a noninteger magnetic flux $\Phi(\vec{r})|_{r\to a^-}$. An approximate expression of the SO term for state n_q with quantum number $(\mu,k;n_q)$ may be derived by rearranging Eq. (6) as

$$\begin{aligned}\frac{\hbar^2}{2m}\left(p_r^2+\frac{1}{r^2}l_+^2+2\eta E_r\frac{1}{r}l_+-k_F^2\right)u_{\mu,k}(r)+|\Delta(r)|v_{\mu,k}(r)\\ =\varepsilon u_{\mu,k}(r)-\frac{\hbar^2}{2m}\left(p_r^2+\frac{1}{r^2}l_-^2-2\eta E_r\frac{1}{r}l_--k_F^2\right)v_{\mu,k}(r)\\ +|\Delta(r)|u_{\mu,k}(r)=\varepsilon v_{\mu,k}(r),\end{aligned} \tag{9}$$

where $l_\pm=\mu\pm(\Phi/\Phi_0+2n_q)/2$, $\eta=e\hbar/4mc^2$, and $\hat{p}_r^2 \equiv \frac{d}{rdr}(r\frac{d}{dr})$. Let us first consider the eigenvalue problem as $r\to a^-$, that is, quasiparticles are confined onto a ringlike region of radius a, and the radial motion can be neglected. The excitation spectrum is given by

$$\varepsilon_n=\frac{\xi_n^+-\xi_n^-}{2}\pm\left[\left(\frac{\xi_n^++\xi_n^-}{2}\right)^2+|\Delta|^2\right]^{1/2}, \tag{10}$$

with $\xi_n^\pm \equiv \frac{\hbar^2}{2ma^2}(\{n\pm[n_q+\Phi/2\Phi_0+\eta aE_r(a)]\}^2-[\eta aE_r(a)]^2-n_F^2)$ and $(\hbar^2\xi^2/2ma^2)(n^2-n_f^2)=\pm\hbar\omega_D$. Therefore, the average energy spectrum of electrons holes at or close to the Fermi level varies with Φ like

$$\frac{\hbar^2}{2ma^2}\{[n_q+\Phi/2\Phi_0+\eta aE_r(a)]^2-[\eta aE_r(a)]^2\}, \tag{11}$$

leading to $\Phi_{so}|_{(\mu,k,n_q)}\sim \eta aE_r[\mathrm{Mod}(\Phi_0)]$. An estimation base on the self-consistent solutions on the SO contribution will be presented in the next section.

B. Magnetic flux associated with the spin-orbit interaction

1. Self-consistent solutions for giant vortex states

We are dealing with a disk of radius a. The BdG Eqs. (6) can be solved separately in each subspace of fixed angular momentum μ.[25] Let $l^\pm(\mu,n_q)=\mu\pm\frac{1}{2}n_q$. We use the normalized Bessel function $\phi_{lk}(r)=\sqrt{2}J_l(\alpha_{l,k}r/a)/aJ_{l+1}(\alpha_{l,k})$ to expand the radial functions: $u_n(r)=\Sigma_k c_{nk}\phi_{l^-(\mu,n_q),k}(r)$ and $v_n(r)=\Sigma_k d_{nk}\phi_{l^+(\mu,n_q),k}(r)$. Here $\alpha_{l,k}$ is the k-th zero of $J_l(x)$, and the integer $k=1,\ldots,N(N=50-80)$. This reduces Eq. (6) to a $2N\times 2N$ matrix eigenvalue problem. [Note that the Fermi wave number or n_F is calculated from, $(\hbar^2/2ma^2)\alpha_{0,n_F}^2=E_F$. We then have $n_F=439$ for $E_F\sim 103$ meV, and $a=4\xi_0$.] The states are classified in terms of their energy eigenvalues. The states that have energy eigenvalue less than $\Delta_0\equiv\max_r[\Delta(r,T,H)]$ for given T and H are known as bound states, whereas those that have energy larger than Δ_0 are named as scattering states. The quasiparticle amplitude of bound states is strongly localized in the vortex core. Figure 1(a) shows the quasiparticle amplitudes $u(r)$ and $v(r)$ corresponding to the lowest eigenvalue $\varepsilon_{1/2}$ $(\mu=1/2, n_q=1)$ at temperature $T=0.08\ \mathrm{K}\ll T_c$. They oscillate with a period of the order of the Fermi wavelength, and their envelope has a maximum at a distance of the order of $r\sim\mu/k_F$. Beyond that distance it decays exponentially. The scattering states become important only at distances larger than the coherence length. Figure 1(b) shows current densities for the lowest energy bound state and the scattering state of $\mu=15/2$, which have opposite signs. The total current density then can be decomposed in terms of contributions of the bound states and scattering states. Close to the vortex core, the current density originating from the bound states is paramagnetic, whereas scattering states contribute a diamagnetic term for $r>\xi$. At distances larger than the penetration depth λ, the paramagnetic and diamagnetic parts essentially cancel, resulting in exponential decay of current density like $e^{-r/\lambda}$.

2. The magnetic flux due to spin-orbit interaction

The pair potentials calculated at temperature $0.8K\sim T_c$ and at 0.08 K are shown in Fig. 1(c). The effective coherence length ξ and penetration depth λ are then found self-consistently. At high temperatures close to T_c, most bound states are thermally activated, and the bound and scattering states contributions to the pair potential become comparable near by the vortex core, resulting in a slow variation of $|\Delta(r)|$. The coherence length ξ_1 derived by fitting the pair potential to the expression of $\Delta(r;T)=\Delta_0(T)\tanh[r/\xi(T)]$ approximates to the (GL) coherence length ξ_0. The SO contribution is then found to be negligible. At low temperatures, e.g., $T=0.08$ K, a very sharp rise of the pair potential in the vicinity of the vortex core is indicated, which is essentially due to the occupation of the low-lying bound states. The pair potential amplitude reaches a value comparable to $\Delta_0(0)\approx 0.345$ meV$=1.268\times10^{-5}$(a.u.) over a distance of the order of $0.1\xi_0=397$(a.u.). Thus, a second expression for coherence length ξ_2 should be defined as $\Delta(r)|_{\mathrm{core}}=\Delta_0(0)r/\xi_2$, leading to $\xi_2-0.1\xi_0$. This rapid variation of the pair potential is reminiscent of a conjecture by Kramer and Pesch.[26] The spatial derivative of pair potential then approximates to

$$\begin{aligned}\partial\Delta/\partial x|_{\mathrm{core}}&\sim(\Delta|_{r_1=0.1\xi_0}-\Delta|_{r_0=0})/(r_1-r_0)=10\cdot\Delta_0/\xi_0\\ &\approx 3.185\times10^{-7}(\mathrm{a.u.}).\end{aligned}$$

The induced electric field strength calculated from expression (1) is $\vec{E}\sim 0.17\times10^{-6}$(a.u.). [Note added: The vortex

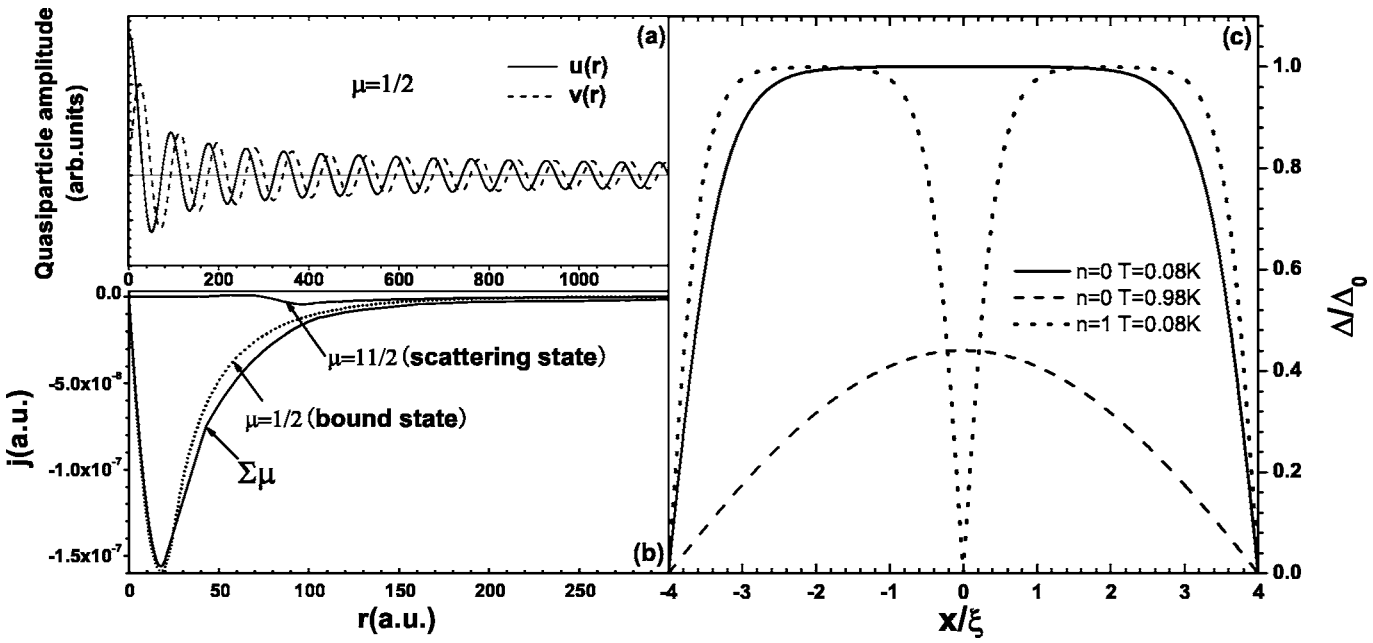

FIG. 1. Spatial distribution of quasiparticle amplitudes $u(r)$ and $v(r)$ corresponding to the lowest eigenvalue $\varepsilon_{1/2}$ (a), self-consistent current density (b) for $n=1$ state, and pair potential(c) for $n=0$ and $n=1$ states at temperatures $T=0.08\ \mathrm{K} \ll T_c$, and $0.8\ \mathrm{K} \sim T_c$.

charge density q_v (in units of a single electron charge) computed from $-4\pi q_v = \nabla \cdot \vec{E}$ is 0.342×10^{-9} (a.u.)$=0.23 \times 10^{-5}\ \mathrm{nm}^{-3}$, and a brief discussion about the feasibility of the experimental observations of the charging effect was presented in Sec. IV] Hence, the SO interaction induced flux (in units of Φ_0) is about $\eta a E_r|_{T\to 0K} \sim 0.3665 \times 10^{-7}$ for a given state $(l,k;n_q)$.

Besides temperature and applied magnetic field, the SO contribution to magnetic flux Φ_{SO} varies with the winding quantum number $l(\mu,n_q)$ and the radial quantum number k of quasiparticles, since the vortex electric field does. The states involved are those that favor to the pairing, that is, those with the quantum number satisfying the inequality $|\alpha_{l,k}^2 \hbar^2/2ma^2 - E_F| \leqslant \hbar\omega_D$. Hence, an upper bound for l is set by $\alpha_{l,1}^2 \hbar^2/2ma^2 = E_F + \hbar\omega_D$, leading to a maximum of $l_{\max} \sim 1578.0$ for the Fermi level $E_F \sim 103$ meV and $\hbar\omega_D = 35$ meV, and $a = 4\xi_0$. In addition, for a fixed angular momentum of the quasiparticles, e.g., $l^{n_f} \sim n_F = 439$, the radial quantum number can span the range of $k(l^{n_f}) \pm 75$ with $k(l^{n_f}) = 243$, that is, about 150 states for the l^{n_f}. The total flux induced by the SO interaction is then a sum running over all favored states, which reads approximately

$$\Phi_{\mathrm{SO}} \sim 2 \cdot \sum_{l,k} \eta a E_r \Big|_{T\to 0K} = 2 \times 1578 \times 150 \times 0.3665 \times 10^{-7} \approx 0.10735, \tag{12}$$

from which one can expect a fractional flux quantum Φ since the total flux $(\Phi + \Phi_{\mathrm{SO}})$ must, as indicated by the necessary condition (8), be quantized in units of Φ_0. Notice that the prefactor in expression (12) comes from the contributions of both l and $-l$ states.

C. The metastable states and saddle states

In type-II superconductors of body, a giant vortex state n that carries flux $n \cdot \Phi_0$ is energetically unfavorable in comparison with the triangle vortex lattice (the Abrikosov lattice) consisting of n vortices that has Φ_0 each. In a finite system, however, a metastable giant vortex is expected. A general solution of the system is a superposition of an infinitivly large number of the giant vortex states that form a complete set for the eigenvalue problem (2). For simplicity, we consider only the coupling between states n_q and n_q+1. We assume

$$u_n(r,\theta) = \sum_k [c_{nk}^{(1)} \phi_{l^-(\mu,n_q),k}(r) e^{i(\mu+n_q/2)\theta} + c_{nk}^{(2)} \phi_{l^-(\mu,n_q+1),k}(r) e^{i[\mu+(n_q+1)/2]\theta}],$$

$$v_n(r,\theta) = \sum_k [d_{nk}^{(1)} \phi_{l^+(\mu,n_q)k}(r) e^{i(\mu-n_q/2)\theta} + c_{nk}^{(2)} \phi_{l^+(\mu,n_q+1)k}(r) e^{i[\mu-(n_q+1)/2]\theta}]. \tag{13}$$

[Note added: We should mention that the selected function does not obey the Neuman boundary condition. But, it would have little effect on the final results. The reason lies mainly on following two points. First, in comparison to the azimuthal component of the supercurrent with its radial component, the former dominates, which implies that the later that is directly proportional to the spatial derivative of the pair potential can be neglected. Second, this approximation is appropriate since the disk radius is not very small (we have chosen $a=4\xi_0$). An algebraic computation shows that the production of the selected function and its derivative drops (2–3) orders at the boundary.]

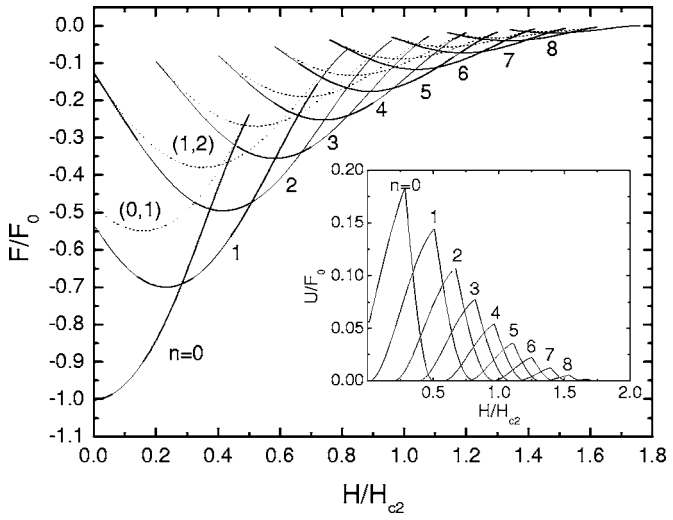

FIG. 2. Free energy for various vortex states of a superconducting disk with $a=4\xi_0$, $h=0.1\xi_0$, and $\lambda=0.30\xi_0$. $F_0 \equiv H_C^2 V/8\pi = \frac{1}{2}N(0)\Delta_0^2(0)V$. The dashed lines show the so-called saddle states that degenerate with the metastable giant vortex states at the penetration (expulsion field) where barriers for state transition $n \to (n+1)[(n+1) \to n]$ vanishes.

This reduces Eq. (2) to a $4N \times 4N$ matrix eigenvalue problem, from which, coupled with Eqs. (3)–(5), the eigenvalue ε_n and eigenvector $[c_{nk}^{(1)}\ c_{nk}^{(2)}\ d_{nk}^{(1)}\ d_{nk}^{(2)}]^T$ and thereby the solutions are solved self-consistently. The free energy F (Note added: There is a formal analogy between the free energy expressed in terms of $|\Delta|^2$ and that described by a wave function ψ of the paired electrons, see, Eqs. (6) and (7) on p. 175 in Ref. 14, for instance.) and the magnetization $M(\Phi) \equiv (\langle \nabla \times A \rangle - H)/4\pi$ can then be computed from the solutions. We plot the field dependences of free energy for various states in Fig. 2 with the solid lines for the giant vortex state, whereas the dashed for the multivortex states.

We consider, for example, state $n_q=1$ and $n_q=2$. As shown in Fig. 2, the upward paraboliclike curve for the multivortex state (1, 2) intersects with the $n_q=1(n_q=2)$ state at the penetration (expulsion) field $H_p^{(1)}$ ($H_e^{(2)}$). We will demonstrate that state transition $1 \to 2(2 \to 1)$ as the magnetic field varies will occur at $H_p^{(1)}$ ($H_e^{(2)}$) due to the charge redistribution, instead of corresponding to field $H_{\rm Sad}^{1 \leftrightarrow 2}$ where state $n_q=1$ degenerates with state $n_q=2$ (without the SO term). Clearly, state $n_q=1(n_q=2)$ then is a metastable state in the magnetic field range $H_{\rm Sad}^{(1 \leftrightarrow 2)} < H < H_p^{(1)}(H_e^{(2)} < H < H_{\rm Sad}^{(1 \leftrightarrow 2)})$. The multivortex state (1,2) that links these metastable states is named as the saddle state. Note that this conclusion remains valid for other n_q values.

D. The barrier for transition $n_q \leftrightarrow n_q+1$

It is well known that a first-order transition between vortex states with different azimuthal quantum number likely occurs at the saddle magnetic field $H_{\rm Sad}^{(n_q \leftrightarrow n_q+1)}$ where the states n_q and n_q+1 degenerate. But if there presents a barrier U, such a first-order transition would take some time that follows an Arrhenius law like $\tau \propto \exp(U/k_BT)$. At sufficiently low temperature such that $U \gg k_BT$, state n_q survives up to the penetration field that is larger than $H_{\rm Sad}^{(n_q \leftrightarrow n_q+1)}$, that is, $H_p^{n_q} > H_{\rm Sad}^{(n_q \leftrightarrow n_q+1)}$. Similarly, with decreasing the magnetic field, the vortex state n_q+1 remains stable until the expulsion field $H_e^{n_q+1} < H_{\rm Sad}^{(n_q \leftrightarrow n_q+1)}$. The origin of barrier, such as the Bean-Livington (BL) model, the vortex pinning by defects, etc., for flux penetration and expulsion has been discussed for decades. These models are essentially based on the London theory, which are then valid only for the vortex motion far from the sample boundary. In addition, the BL barrier is found independent on the vortex core energy,[27] and it seems unlikely accounting for vortex dynamics in mesoscopic superconductors. We believe the charge redistribution around vortices can provide a barrier. We present a plausible argument.

The charging of vortices has two consequences at least. First it induces a radial electric field that provides the force necessary for the circular motion of quasiparticles in a vortex, which has to overcompensate the Lorentz force on those carriers for a stable vortex structure. Second, there presents an extra force on a moving vortex because of the charge redistribution around the vortex. A *charged vortex* (with charge density q_v) moving with the velocity v_q yields a current density $\vec{j}_v = q_v \vec{v}_q$. Charge neutrality then requires a backflowing supercurrent $-j_v$ that exerts a Lorentz or Magnus force, $-q_v \Phi_q \vec{v}_q \times \vec{n}$, on the vortex. Where $\vec{n}$ is a unit vector in the direction of the vortex axis. This force drives vortices parallel ($q_v > 0$) or antiparallel ($q_v < 0$) to the electric field when the charging vortex moves circularly, and it forces the charged vortex core circulating about the disk axis when the initial $\vec{v}_q$ directs along the radial axis, which makes sense to speak of a barrier for flux penetration and expulsion.

Figure 3(a) shows charge distribution for state $n_q=1$, the free energy F for state $n_q=1$, $n_q=2$ and saddle state (1,2) of the vortex charge free case in Fig. 3(b), and the associated electrostatic energy E_q due to charge redistribution in Fig. 3(c). Clearly, with field increase up to $H_{\rm Sad}^{1 \leftrightarrow 2}$, state transition $1 \to 2$ would unlikely occur since the SO interaction contributes a larger energy to the state $n_q=2$ in comparison with that to $n_q=1$. The system then remains in the *metastable* $n_q=1$ state for $H > H_{\rm Sad}^{(1 \leftrightarrow 2)}$ up to the critical field $H_c^{n_q \to n_q+1}$ where the meatastable state degenerates with the saddle state. Remarkably, we find at the field $H_p^{(1)}$: $E_{12}(H_p^{(1)}) + F_{12}(H_p^{(1)}) = E_1(H_p^{(1)}) + F_1(H_p^{(1)})$.

In addition, at $H_e^{(2)}$: $E_{12}(H_e^{(2)}) + F_{12}(H_e^{(2)}) = E_2(H_e^{(2)}) + F_2(H_e^{(2)})$.

These results demonstrate that $H_p^{(1)}$ ($H_e^{(2)}$) are indeed the critical field for vortex penetration (expulsion) or a transition $1 \to 2$ $(2 \to 1)$ occurs due to thermal instability of the system.

To find out the barrier, one needs a time-dependent model, e.g., the time-dependent BdG model that includes the charge redistribution, which will be presented elsewhere. Here, we present a phenomenological approach. As discussed above, in *energy space* a multivortex state (n_q, n_q+1) is a *saddle* state that links the metastable states n_q and n_q+1. It may also be treated as a transit state dynamically. Figure 4 shows vortex cores of state (1,2) distribution varying with magnetic field. At the saddle field $H_{\rm Sad}^{1 \leftrightarrow 2}$, one core locates at the disk

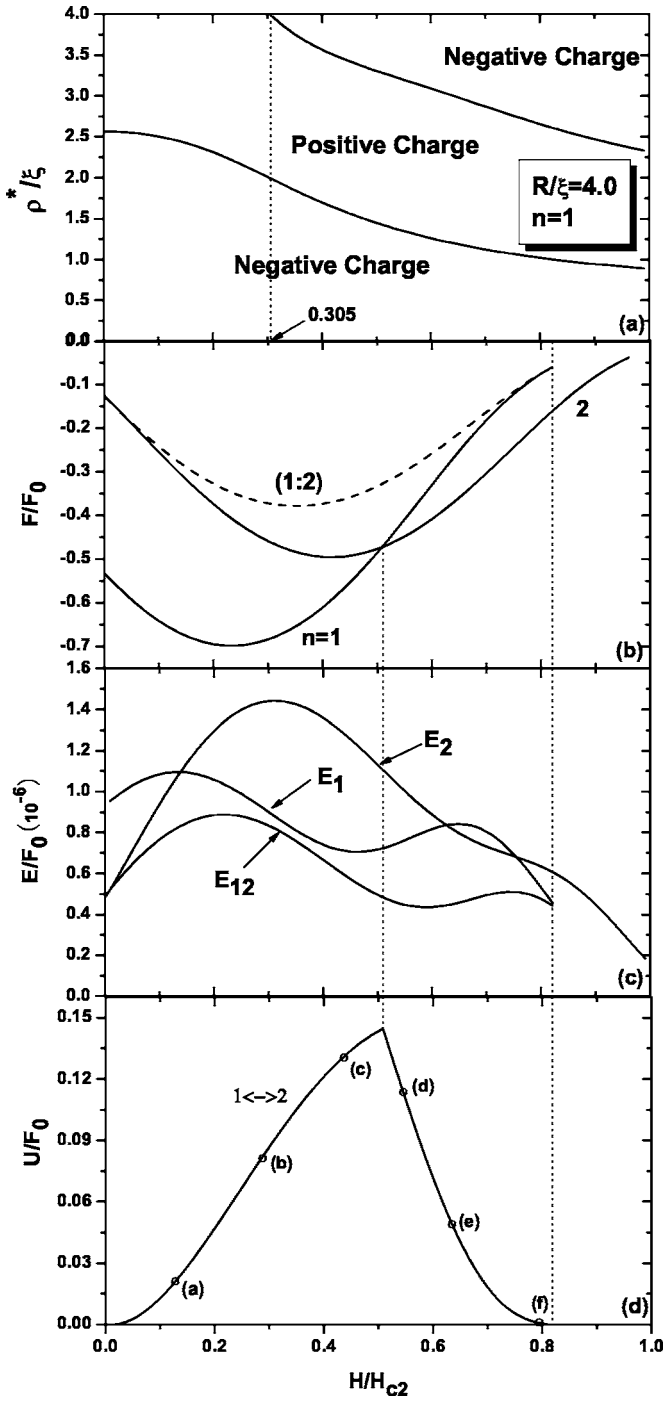

FIG. 3. Vortex charge distribution (a) (ρ^* measures the distance from the disk center where vortex charge sign reversal occurs.), the free energy of charge free case (b), the spin-orbit contribution to the state energy (c), and the barrier (d) for transition $1 \leftrightarrow 2$ varying with magnetic field. State transition occurs only when $F_{(n,n+1)}+E_{(n,n+1)}=F_n+E_n$.

center, another one at the outer edge of the disk. Remember that the system is now in the $n_q=1(or\ n_q=2)$ state. A core of a transient state could accommodate somewhere away from the disk center simply because there presents a barrier that prevents its jumping on to (out of) disk center. The height of the barrier is then the energy difference between the saddle

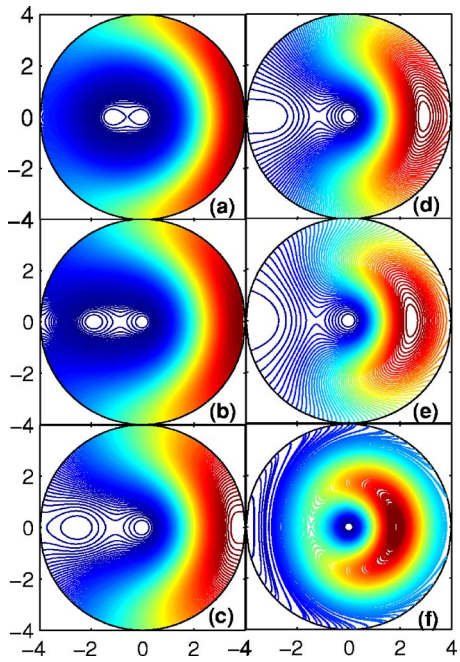

FIG. 4. (Color online) Contour plots of pair potential, indicating how a vortex core (the circlelike white zone) where amplitude of pair potential vanishes is expelled out of the multivortex (1,2) state with magnetic field increasing from (a) to (f) [see Fig. 3(d)].

state and the corresponding metastable state(s). Figure 3(d) shows the barrier for transition $1 \leftrightarrow 2$. Similarly, the barriers for transition $n_q \leftrightarrow n_q+1$ that are defined as the energy difference between state (n_q, n_q+1) and state n_q (n_q+1) for $H > H_{\mathrm{Sad}}^{n_q \leftrightarrow n_q+1} (H < H_{\mathrm{Sad}}^{n_q \leftrightarrow n_q+1})$ are plotted in Fig. 2 (the inset).

It is interesting to note that with a field increase from $H_{\mathrm{Sad}}^{n_q \leftrightarrow n_q+1}$ up to $H_p^{(n_q)}$ where $U_B \to 0$ state transition $n_q \to n_q+1$ occurs accompanied remarkably with an increase in the sample magnetization shown by the thick solid arrows in Fig. 5. Thus, the total flux penetration through the superconducting disk will indicate a negative jump.

IV. CLOSING REMARKS

We show that magnetic flux carried by vortices may differ from the flux quanta Φ_0 because of the charged vortex induced spin-orbit coupling that generates an additional geometric (the ac-like) phase to the wave function. The fractional flux quanta (the AB flux) is expected since the wave function phase must be quantized [Mod(2π)]. Furthermore, we find that the spin-orbit coupling would in principle depress the first-order transition between giant vortex states, and the system is expected to evolve along metastable giant vortex states. Consequently, with a magnetic field increase, sample's magnetization is expected to increase as state transition occurs since magnetization for the preexisting state drops significantly, implying negative flux jump.

Finally, we present a brief discussion about the feasibility of the experimental observations of the vortex charging effect. One can examine the $T_C(H)$ phase boundary of a single connected sample (a cylinder or a disk) in an axial magnetic

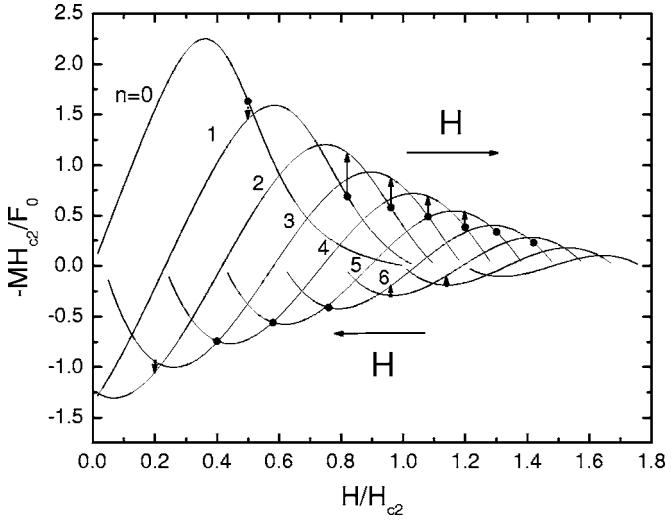

FIG. 5. Magnetization response for the superconducting Al disk. The solid arrows show that vortex number increasing could possibly result in flux expulsion, whereas flux inside the superconductor increases when a vortex leaves has not been seen, which are consistent with the experiments of Geim *et al.* (Ref. 1).

field. As in the original Little-Parks experiment for a multiply connected thin-wall Tin microcylinder[28] an oscillation in $T_C(H)$ will occur. But in this case, the oscillation period is expected to decrease as H increases due to the presence of SO contribution. Actually, moving along the $T_C(H)$ boundary, the pair potential concentrates more and more near the sample edge, implying a larger spin-orbit contribution because of a sharper potential distribution, and a less AB-like flux or a noninteger flux penetration. On the other hand, for the multiply connected case (a thin cylindric shell or a ring), the giant vortex core locates at the center of the sample and an almost uniform pair potential over the shell is found, leading to a significant decrease in the SO contribution and the oscillations in T_c are perfectly periodic with Φ. [Note added: Similar results would be expected when one works in the framework of the GL theory by considering the fact that there is no additional flux should be included for the shell, whereas such a contribution would be included for the disk.] For an experimental verification of this predictions, the readers can refer to Ref. 29. Furthermore, for a direct detection of the vortex field, one may envisage the classic geometry for the observation of vortices via the Bitter-decoration technique, with the superconductor filling half space, e.g., $z<0$ and penetrated by a magnetic field $\vec{B}\|\hat{z}$. The resulting vortex line is charged up due to particle-hole asymmetry, which in turn generated an electric field or a surface electric dipole that can be detected by sweeping a tip over sample surface. Blatter *et al.*[30] discussed the detection of vortex field in type-II superconductors by the scanning tunneling microscopy. Also, the vortex charge in high-temperature superconductor (HTSC) $YBa_2Cu_3O_7$ was detected by nuclear magnetic resonance method.[31] It has been shown[16] that the vortex charge due to the opening of the energy gap or the transition of a system to superconducting is in the order of $\Delta/E_F \sim (m/2\hbar^2\xi^2\pi^2\Delta)^{-1}$ [We have used the expression: $E_F \sim m/2\hbar^2\pi^2\Delta^2\xi^2$ for a metallic superconductor in the clean limit (cf. Ref. 14). This ratio is then orders smaller for typical metallic superconductors than that of HTSC, for which the vortex charge is in the order of $10^{-3}e$ when $\xi(0)\sim 5$ Å. Consequently, above mentioned techniques would be challenged because of limited accuracy. Recently, Geim *et al.* developed the ballistic Hall megnetometry,[32] and abnormal magnetic responses in mesoscopic disks of metallic superconductor (aluminum) have been signaled by using this technique,[1] which sheds lights on experimental detection the vortex charge in mesoscopic metallic superconductors. In addition, this technique will be useful to detect vortex charge field in type-II metallic superconductors, e.g., the niobium-alloy material, Nb_3Sn where[33] the coherence length is $\sim$4 nm, and the critical temperature $T_C=18$ K, or $\Delta(0)\sim 4$ meV, from which a value of Δ/E_F is estimated in the order of 3.5×10^{-2} that is comparable to the value of 10^{-1} for typical HTSCs.[34–38]

Note added: The theoretical calculations without involving the SO term suggested that the $n_q+1\rightarrow n_q$ transition would occur at the field less than the magnetic field where magnetizations for those two states intersect, implying a positive jump with decreasing magnetic field (see, Fig. 3 of Ref. 1). The positive flux jump with decreasing magnetic field (but its orientation unchanged) has, however, not been found in our simulations. We can prove that the modified Bogoliubov-de-Gennes Eqs. (1) are invariant under the transformation $u\rightarrow v^*$, $v\rightarrow -u^*$, and $\varepsilon\rightarrow -\varepsilon$, which relates an eigenstate to its time-reversal counterpart.[24] Clearly, decreasing field intensity, whereas its orientation remains unchanged, does not physically match with the time-reversal operation. Remember that the SO term is time-reversal invariant. Therefore, differences in the system magnetic response would be expected for increase with decrease field. For increasing field (see Fig. 5), the magnetization of a n_q state saturates first and drops quickly beyond the saddle point field, which becomes less than that of the succeeding n_q+1 state at $H_p^{(n)}$. Thus, the sample magnetization increases as $n_q\rightarrow(n_q+1)$ state transition occurs, yielding a negative flux jump at $H_p^{(n_q)}$. For decreasing field, however, the transition field $H_e^{(n_q+1)}$ locates very close to the valley of the magnetization curve for the preexisting n_q+1 state, where the total screening current flow direction reversal is expected. Clearly, the vortex field exerts now a Lorentz force on the vortex line that attempts to expel magnetic flux out of the sample. Therefore, transitions with magnetic field decrease occur at $H_e^{(n_q+1)}$ and would be no positive flux jump so long as the applied field orientation remains unchanged. Indeed, "flux inside a superconductor increases when a vortex leaves has not been seen" in the experiments of Geim *et al.*[1]

ACKNOWLEDGMENT

This work is supported by the National Natural Science Foundation of China (Grant No. 60371033).

[1] A. K. Geim, S. V. Dubonos, I. V. Grigorieva, K. S. Novoselov, F. M. Peeters, and V. A. Schweigert, Nature (London) **407**, 55 (2000).
[2] H. J. Fink and V. Grunfeld, Phys. Rev. B **22**, 2289 (1980).
[3] B. J. Baelus, F. M. Peeters, and V. A. Schweigert, Phys. Rev. B **63**, 144517 (2001).
[4] J. Berger, Phys. Rev. B **67**, 014531 (2003).
[5] D. Y. Vodolazov, F. M. Peeters, S. V. Dubonos, and A. K. Geim, Phys. Rev. B **67**, 054506 (2003).
[6] A. K. Geim, S. V. Dubonos, J. J. Palacios, I. V. Grigorieva, M. Henini, and J. J. Schermer, Phys. Rev. Lett. **85**, 1528 (2000).
[7] V. A. Schweigert and F. M. Peeters, Phys. Rev. Lett. **83**, 2409 (1999).
[8] J. J. Palacios, Phys. Rev. Lett. **84**, 1796 (2000).
[9] C. P. Bean and J. B. Livingston, Phys. Rev. Lett. **12**, 14 (1964).
[10] J. Bardeen, Phys. Rev. Lett. **7**, 162 (1961).
[11] V. L. Ginzburg, Sov. Phys. JETP **15**, 207 (1962).
[12] B. S. Deaver, Jr. and W. M. Fairbank, Phys. Rev. Lett. **7**, 43 (1961); A. L. Fetter and J. D. Wackecka, *Quantum Theory of Many Particle Systems* (McGraw-Hill, New York, 1971).
[13] N. Byers and C. N. Yang, Phys. Rev. Lett. **7**, 46 (1961).
[14] P. G. de Gennes, *Superconductivity of Metals and Alloys* (Benjamin, Inc., New York, 1966).
[15] G. Blatter, M. Feigel'man, V. Geshkenbein, A. Larkin, and A. van Otterlo, Phys. Rev. Lett. **77**, 566 (1996).
[16] D. I. Khomskii and A. Freimuth, Phys. Rev. Lett. **75**, 1384 (1995).
[17] J. Kolacek, P. Lipavsky, and E. H. Brandt, Phys. Rev. Lett. **86**, 312 (2001).
[18] N. Hayashi, T. Isoshima, M. Ichioka, and K. Machida, Phys. Rev. Lett. **80**, 2921 (1998).
[19] Ken-ichi Kumagai, Koji Nozaki, and Yuji Matsuda, Phys. Rev. B **63**, 144502 (2001).
[20] S. V. Yampolskii, B. J. Bealus, F. M. Peeters, and J. Kolacek, Phys. Rev. B **64**, 144511 (2001).
[21] M. Eschrig, J. A. Sauls, and D. Rainer, Phys. Rev. B **60**, 10447 (1999).
[22] Y. Aharonov and A. Casher, Phys. Rev. Lett. **53**, 319 (1984).
[23] C. Carroli, P. G. de Gennes, and J. Matricon, Phys. Lett. **9**, 307 (1964).
[24] The proof of the theorem is straightforward (see. Ref. 14), since the spin-orbit coupling term is gauge invariant.
[25] F. Gygi and M. Schlueter, Phys. Rev. B **43**(10), 7609 (1991).
[26] L. Kramer and W. Pesch, Z. Phys. **269**, 59 (1974).
[27] A. I. Buzdin and J. P. Brison, Phys. Lett. A **196**, 267 (1994).
[28] W. A. Little and R. D. Parks, Phys. Rev. Lett. **9**, 9 (1962).
[29] V. V. Moshchalkov, L. Gielen, C. Strunk, R. Jonckheere, X. Qiu, C. Van Haesendonck, and Y. Bruynseraede, Nature (London) **373**, 319 (1995).
[30] G. Blatter, M. Feigel'mann, V. Geshkenbein, A. Larkin, and A. Van Otterlo, Phys. Rev. Lett. **77**, 566 (1996).
[31] K. I. Kumagai, K. Nozaki, and Y. Matsuda, Phys. Rev. B **63**, 144502 (2001).
[32] A. K. Geim, J. G. S. Lok, S. V. Gubonos, J. C. Maan, L. Theil-Hansen, and P. E. Lindelof, Appl. Phys. Lett. **71**, 2379 (1997).
[33] A. K. Geim, I. V. Grigorieva, S. V. Dubonos, J. G. S. Lok, J. C. Mann, A. E. Filippov, and F. M. Peeters, Nature (London) **390**, 259 (1997).
[34] V. Guritanu, W. Goldacker, F. Bouquet, Y. Wang, R. Lortz, G. Goll, and A. Junod, Phys. Rev. B **70**, 184526 (2004).
[35] S. H. Pan, E. W. Hudson, A. K. Gupta, K.-W. Ng, H. Eisaki, S. Uchida, and J. C. Davis, Phys. Rev. Lett. **85**, 1536 (2000).
[36] M. Matsumoto and R. Heeb, Phys. Rev. B **65**, 014504 (2002).
[37] M. Machida and T. Koyama, Phys. Rev. Lett. **90**, 077003 (2003).
[38] Y. Aharonov and D. Bohm, Phys. Rev. **115**, 485 (1959).